IEEE Access
Multidisciplinary | Rapid Review | Open Access Journal

Received December 29, 2020, accepted January 18, 2021, date of publication January 26, 2021, date of current version February 8, 2021.

Digital Object Identifier 10.1109/ACCESS.2021.3054807

A Method of Reweighting the Sensing Matrix for Compressed Sensing

LEI SHI[1], GANGRONG QU[1], AND QIAN WANG[2]
[1]School of Science, Beijing Jiaotong University, Beijing 100044, China
[2]School of Science, Tianjin University of Commerce, Tianjin 300134, China

Corresponding author: Gangrong Qu (grqu@bjtu.edu.cn)

This work was supported in part by the National Natural Science Foundation of China under Grant 61931003 and Grant 61671004.

ABSTRACT In compressed sensing, a small enough restricted isometry constant (RIC) of the sensing matrix satisfying the restricted isometry property (RIP) is the powerful guarantee on the precise reconstruction of a sparse discrete signal. Under a certain condition, the RIC can be improved by weighting the sensing matrix so that its all nonzero singular values become the same, i.e., the condition number of the new sensing matrix is 1. In this article, by multiplying the linear system $\boldsymbol{A}^T\boldsymbol{A}\boldsymbol{x} = \boldsymbol{A}^T\boldsymbol{y}$ by a matrix related to $\boldsymbol{A}^T\boldsymbol{A}$ and repeating the process many times, we propose a method of reweighting the sensing matrix to improve the condition number of sensing matrix so as to improve its RIC, prove that the condition number tends to 1 as the weighting times approaches infinity monotonically, and then obtain an RIC improvement model equivalent to the original CS model. For the improvement model, we use the algorithms of orthogonal matching pursuit, iterative hard thresholding and $L_{1/2}$-regularisation to recover sparse signals, and verify the superiority of the proposed algorithms by using different existing sensing matrices for CS experiments.

INDEX TERMS Compressed sensing, restricted isometry constant, sensing matrix.

I. INTRODUCTION

Compressed sensing (CS) aims to recover a sparse discrete signal, $\boldsymbol{x}$, from an underdetermined sampling observed data, $\boldsymbol{y}$, through a basic model

$$\boldsymbol{A}\boldsymbol{x} = \boldsymbol{y} \tag{1}$$

where $\boldsymbol{A} \in \mathbb{C}^{M\times N}(M \ll N)$, a known sensing matrix, models the sensing progress [1]. CS has been exploited in many practical fields such as radar imaging, cryptography, multi-sensor signal processing, signal processing and communication [2]–[6].

One of the key problems in CS is the design of recovery algorithm. CS mainly includes three categories of algorithms: optimization, greedy, and thresholding-based methods. The existing classical algorithms include the orthogonal matching pursuit (OMP) [7], the iterative hard thresholding (IHT) [8], $L_{1/2}$-regularization algorithm ($L_{1/2}$R) [9], L_p-Minimization algorithm [10], and the Quasi-Newton Iterative Projection Algorithm [11].

Definition 1.1 [12]: The restricted isometry constant (RIC) $\delta_s = \delta_s(\boldsymbol{A})$ of the matrix $\boldsymbol{A}$ with restricted isometry property (RIP) of order s is defined to be a smallest positive number such that

$$C_s(1-\delta_s)||\boldsymbol{x}||_2^2 \le ||\boldsymbol{A}\boldsymbol{x}||_2^2 \le C_s(1+\delta_s)||\boldsymbol{x}||_2^2 \tag{2}$$

for some positive number C_s and all s sparse vectors $\boldsymbol{x} \in \mathbb{C}^N$. The ability of these algorithms to recover accurately is closely associated with δ_s, the smaller the δ_s, the more accurate the results.

Recently, people devoted to studying the constraints on δ_s of $\boldsymbol{A}$ to ensure the valid reconstruction of s sparse signals. Song *et al.* [13] established the condition, $\delta_{3s} < 0.4859$, to ensure the recovery of any s-sparse signals by the subspace pursuit method. Wang and Qu [14] presented that OMP can recover exactly any s sparse signals under the condition $\delta_{s+1} < 1/\left(\sqrt{s}+1\right)$. For the covariance-assisted matching pursuit algorithm, Ge *et al.* [15] developed a sufficient condition of exact support recovery of any s sparse signals, $\delta_{s+1} < 2/\left(\sqrt{(\sqrt{s}+2)^2 + 2(1-\sqrt{s+1})} + \sqrt{s+1}+1\right)$. Wu and Chen [10] indicated that

$$\delta_{2s} < \frac{2^{\frac{2}{p}-2}}{p(2-p)^{\frac{2}{p}-1} + 2^{\frac{2}{p}-2}} - \frac{p(2-p)^{\frac{2}{p}-1}}{4p(2-p)^{\frac{2}{p}-1} + 2^{\frac{2}{p}}}$$

The associate editor coordinating the review of this manuscript and approving it for publication was Pietro Savazzi.

suffices for the exact sparse recovery of L_p-minimization. For the multiple orthogonal least squares method allowing multiple l indices to be chosen per iteration, Wang and Li [16] demonstrated that any s sparse signals can be successfully recovered via this method under the condition that the sensing matrix $\boldsymbol{A}$ has unit ℓ_2-norm columns satisfying RIP of order ls with $\delta_{ls} < 1/\left(\sqrt{s/l}+2\right)$. Li *et al.* [17] improved the bound further to $\delta_{ls+1} < 1/\left(\sqrt{s/l}+2\right)$. Liu *et al.* [18] proven that alternating projection method can reconstruct any s sparse signals if $\delta_{2s} + \left(1-\sqrt{2}/4\right)\sigma^2_{m-2s+1} < 1$, where σ_{m-2s+1} is the $(m-2s+1)$ *th* singular value of $\boldsymbol{A}$ with $rank(\boldsymbol{A}) = m$.

The other of the key problems in CS is the design of the sensing matrix $\boldsymbol{A}$. Over the years, there have been many references on the sensing matrices in (1). Candes and Tao [19] proved that Gaussian random matrices satisfy the RIP with overwhelming probability. Abolghasemi *et al.* [20] provided a gradient descent method to optimize the Gaussian random matrices in CS and the experimental results showed that the optimized matrices can improve reconstruction quality than before. Saligrama [21] presented a deterministic construction of Toeplitz matrices and stated its feasibility in CS. Li *et al.* [22] indicated that the matrix with small coherence cannot be with a large δ_s. So people usually also design a sensing matrix by reducing the coherence value. Li *et al.* [23] designed a projection matrix with the prior information of the reconstructed sparse signal and proved that the designed matrix can reduce local cumulative coherence so that improving the sparse signal recovery rate. Ebian *et al.* [24] introduced a modified regular parity check matrix with a small mutual coherence and showed the matrix has a better reconstruction performance on the CS in cognitive radio networks than Gaussian random matrix.

In these literatures, the sensing processes are unfixed and determined by the designed sensing matrices. However, sometimes the sensing process is fixed and the sensing matrix determined by the sensing process is immutable, once the δ_s of the sensing matrix is large, it is very hard to implement a valid s sparse recovery in CS. For the fixed sensing matrix $\boldsymbol{A}$ in (1), denote its singular value decomposition (SVD) as, $\boldsymbol{A} = \bar{\boldsymbol{U}}\begin{pmatrix}\boldsymbol{S} & \boldsymbol{0}\\ \boldsymbol{0} & \boldsymbol{0}\end{pmatrix}\bar{\boldsymbol{V}}^T$, where $\boldsymbol{S} = diag\{\sigma_1, \sigma_2, \cdots, \sigma_r\}$ and the singular values satisfy $\sigma_1 \geq \sigma_2 \geq \cdots \geq \sigma_r > 0$. To improve the δ_s, authors [14] presented a weighted method, in which left multiply (1) by matrix $\begin{pmatrix}\boldsymbol{S^{-1}} & \boldsymbol{0}\\ \boldsymbol{0} & \boldsymbol{I}\end{pmatrix}\bar{\boldsymbol{U}}^T$, where $\boldsymbol{I}$ is a unit matrix and $\boldsymbol{S^{-1}} = diag\left\{\frac{1}{\sigma_1}, \frac{1}{\sigma_2}, \cdots, \frac{1}{\sigma_r}\right\}$, and gave two important conclusions. One conclusion is that the smaller $\frac{\mu^s_{\max}}{\mu^s_{\min}}$ (the ratio of the maximum eigenvalues of the Gram matrices of all the submatrices composed of s columns of the sensing matrix to the minimum of these eigenvalues), the smaller is the RIC. The other is that $\frac{\mu^s_{\max}}{\mu^s_{\min}}$ can be improved, under the condition (6), by weighting the sensing matrix to equalize all its singular values (i.e., the condition number becomes 1). The weighted method of [14] had been used for some sparse signal recoveries in CS with a fixed sensing matrix and the results obtained by the weighted recovery algorithms are preferable to those acquired by the direct recovery algorithms. The weighted method requires the SVD with a lot of numerical computations and the reciprocals of all singular values, which will lead to large round-off errors especially for those appropriately small singular values.

In [25], through multiplying the linear system $\boldsymbol{A^TAx} = \boldsymbol{A^Ty}$ with the same least square solution as the equation (1) by a matrix related to $\boldsymbol{A^TA}$ and repeating the process many times, we introduced a reweighted method of improving the condition number and improved the reconstructed results of band-limited signals. We also applied elementarily the reweighted method for the recovery of the blind multiband signals [26].

In this article, we apply the reweighted method to improve the RIC of the sensing matrix for general CS. The reweighted method can improve condition number of $\boldsymbol{A^TA}$ [25]. By using the reweighted method to weight the norm equation of the original CS model (1), a new CS model (19) equivalent to (1) is obtained. We prove that the RIC of $\boldsymbol{\Psi_n}$, i.e., the new sensing matrix in (19), is improved under the assumption condition of [14]. Meanwhile, we prove that the result of improving RIC also holds after expanding the weighted parameter from $1 < a_n < 2$ to $a_n > 1$. Compared with the weighted method of [14], the reweighted method only needs the maximum eigenvalue of the sensing matrix and its weighted matrix has a small condition number, so it is simpler and more stable. Besides we also establish the reweighted OMP, IHT and $L_{1/2}$R recovery algorithms respectively. We use Gaussian random matrix, Toeplitz matrix and uniform random matrix as the sensing matrix to carry out the CS experiments of the general one-dimensional sparse signal recovery respectively and verify the superiority of the proposed algorithms by comparing with the direct recovery algorithms and the algorithms of [14]. Besides, the reweighted OMP recovery algorithm is also used for the CS problem of computed tomography (CT) and gets a valid reconstruction result.

The remaining of this article is organized as follows. In section II, we introduce several necessary known results. In section III, we establish a complete theoretical analysis of improving RIC for the reweighted method. In section IV, we give several reweighted recovery algorithms and implement experiments. In section V, we give a conclusion.

II. PRELIMINARIES

In this section, we give some preliminary results.

Definition 2.1: Denote $\mu_{\max}$ and $\mu_{\min}$ are the largest singular value of $\boldsymbol{A}$ and the smallest nonzero singular value respectively, then the condition number of $\boldsymbol{A}$ is

$$\mathcal{K}(\boldsymbol{A}) = \frac{\mu_{\max}}{\mu_{\min}}. \tag{3}$$

Theorem 2.1 [14]: Suppose a matrix, $\boldsymbol{A}$, satisfies the RIP of order s, then the left-hand and right-hand side equalities in (2) can be attained, respectively, if we let

$$C_s = \frac{\mu^s_{\max} + \mu^s_{\min}}{2}, \quad \delta_s(\boldsymbol{A}) = 1 - \frac{2}{\frac{\mu^s_{\max}}{\mu^s_{\min}} + 1}. \tag{4}$$

Obviously, the smaller value of $\frac{\mu^s_{\max}}{\mu^s_{\min}}$, the smaller is $\delta_s(\boldsymbol{A})$.

Algorithm 1 OMP Algorithm

Input: observed data $\boldsymbol{y}$, Sensing matrix $\boldsymbol{A}$, sparsity s.
Initialization: $T^0 = \emptyset, \boldsymbol{x^0} = \boldsymbol{0}$;
Iteration: Repeat until a stopping criterion is met at $k = \bar{k}$
1: $T^{k+1} = T^k \bigcup \{j_{k+1}\}$,
2: $j_{k+1} = \arg\max_{j \in [1,\ldots,s]} \left\{ \left| \left(\boldsymbol{A^T} \left(\boldsymbol{y} - \boldsymbol{A}\boldsymbol{x^k} \right) \right)_j \right| \right\}$,
3: $\boldsymbol{x^{k\mathcal{C}1}} = \arg\min_{z \in \mathbb{C}^n} \left\{ \|\boldsymbol{y} - \boldsymbol{A}\boldsymbol{z}\|_2 \right\}$, $\sup(z) \subseteq T^{k+1}$.
Output: $\boldsymbol{x^{k_1}}$

Algorithm 2 IHT Algorithm

Input: observed data $\boldsymbol{y}$, Sensing matrix $\boldsymbol{A}$, sparsity s.
Initialization: $\boldsymbol{x^0} = \boldsymbol{0}$;
Iteration: Repeat until a stopping criterion is met at $k = \bar{k}$
1: $\boldsymbol{x^{k\mathcal{C}1}} = H_s \left(\boldsymbol{x^k} + \boldsymbol{A^T} \left(\boldsymbol{y} - \boldsymbol{A}\boldsymbol{x^k} \right) \right)$, where $H_s(\boldsymbol{x})$ means setting all but the largest (in magnitude) s elements of $\boldsymbol{x}$ to zero.
Output: $\boldsymbol{x^{k_1}}$

Algorithm 3 $\mathrm{L}_{1/2}$R Algorithm

Input: observed data $\boldsymbol{y}$, Sensing matrix $\boldsymbol{A}$, sparsity s.
Initialization: $\boldsymbol{x^0} = \boldsymbol{0}$, $\lambda_0 = 0.5$ and $u = \frac{0.09}{\|A\|^2}$;
Iteration: Repeat until a stopping criterion is met at $k = \bar{k}$
1: $\boldsymbol{x^k} = \boldsymbol{x^k} + u\boldsymbol{A^T} \left(\boldsymbol{y} - \boldsymbol{A}\boldsymbol{x^k} \right)$,
2: $\lambda_k = \min \left(\lambda_{k-1}, \frac{\sqrt{96}}{9} \|A\|^2 \left| [\boldsymbol{x^k}]_{s+1} \right|^{\frac{3}{2}} \right)$; where $\left[\boldsymbol{x^k}\right]_{s+1}$ is the $(s+1)$th largest component of $\boldsymbol{x^k}$ in magnitude.
3: $\boldsymbol{x^{k\mathcal{C}1}} = H_{\lambda_k u, \frac{1}{2}} \left(\boldsymbol{x^k} \right)$,
4: **if** $\left| \boldsymbol{x^k}_i \right| > \frac{\sqrt[3]{54}}{4} (\lambda_k u)^{\frac{2}{3}}$ **then**
5: $H_{\lambda_k u, \frac{1}{2}} \left(\boldsymbol{x^k}_i \right) = \frac{2\boldsymbol{x^k}_i}{3} \left[1 + \cos \left(\frac{2\pi}{3} - \frac{2}{3} \arccos \left(\frac{\lambda_k u}{8} \left(\frac{|\boldsymbol{x^k}_i|}{3} \right)^{-\frac{3}{2}} \right) \right) \right]$;
6: **else**
7: $H_{\lambda_k u, \frac{1}{2}} \left(\boldsymbol{x^k}_i \right) = 0$.
8: **end if**
Output: $\boldsymbol{x^{k_1}}$

Theorem 2.2 [14]: For $s \leq r$, r is the rank of the sensing matrix $\boldsymbol{A}$. Denote the weighted sensing matrix obtained by the weighted method of [14] by $\boldsymbol{A_{svd}} = \begin{pmatrix} \boldsymbol{I} & 0 \\ 0 & 0 \end{pmatrix} \bar{\boldsymbol{V}}^T$ (obviously, the all nonzero singular values of $\boldsymbol{A_{svd}}$ are the same), then

$$\frac{\mu^s_{\max}(\boldsymbol{A})}{\mu^s_{\min}(\boldsymbol{A})} > \frac{\mu^s_{\max}(\boldsymbol{A_{svd}})}{\mu^s_{\min}(\boldsymbol{A_{svd}})} \tag{5}$$

if

$$\frac{\sigma_1}{\sigma_s} > \frac{1}{\|\boldsymbol{\omega_{T_0}}\|_2} \sqrt{\frac{\mu^s_{\max}(\boldsymbol{A_{svd}})}{\mu^s_{\min}(\boldsymbol{A_{svd}})}}, \tag{6}$$

where $T_0 = \arg\max_{|T|=s} \|\boldsymbol{\omega_T}\|_2$, $T \subset \{1, 2, \ldots, n\}$ with $|T| = s$ and $\boldsymbol{\omega}$ is the first row of $\bar{\boldsymbol{V}}^{\boldsymbol{T}}$.

In the proof of Theorem 2.2, authors have proved that $\mu^s_{\max}(\boldsymbol{A}) \geq \sigma_1^2 \|\boldsymbol{\omega_{T_0}}\|_2^2$ and $\mu^s_{\min}(\boldsymbol{A}) \leq \sigma_s^2$, then $\frac{\mu^s_{\max}(\boldsymbol{A})}{\mu^s_{\min}(\boldsymbol{A})} \geq \frac{\sigma_1^2 \|\boldsymbol{\omega_{T_0}}\|_2^2}{\sigma_s^2}$. So for a weighted method, if only its weighted sensing matrix, $\bar{\boldsymbol{A}}$, satisfies $\frac{\sigma_1^2 \|\boldsymbol{\omega_{T_0}}\|_2^2}{\sigma_s^2} > \frac{\mu^s_{\max}(\bar{\boldsymbol{A}})}{\mu^s_{\min}(\bar{\boldsymbol{A}})}$, i.e., the assumption (6), the inequality (5) holds and the RIC is improved.

For the original CS model (1), the frameworks of the existing OMP, IHT and $\mathrm{L}_{1/2}$R algorithms are given in **Algorithms** 1, 2 and 3 respectively. The process of $\mathrm{L}_{1/2}$R algorithm is complex, we do not state it in detail here and some specific calculation formulas are shown in [9].

III. THE REWEIGHTED METHOD OF IMPROVING RIC

In this section, we give a reweighted method and prove that the RIC is improved under a certain condition. The reweighted method is as follows,

$$\boldsymbol{A_0} = \boldsymbol{A^T A}, \quad \boldsymbol{y_0} = \boldsymbol{A^T y}, * \tag{7a}$$

$$\boldsymbol{V_n^{-1}} = a_n \mu_{n-1,1} \quad \boldsymbol{I} - \boldsymbol{A_{n-1}}, \text{ for } a_n > 1, \tag{7b}$$

$$\boldsymbol{A_n} = \boldsymbol{V_n^{-1} A_{n-1}}, \quad \boldsymbol{y_n} = \boldsymbol{V_n^{-1} y_{n-1}}, \tag{7c}$$

where a_n are weighted parameters and $\mu_{n,1}$ are the largest positive eigenvalues of $\boldsymbol{A_n}$, $n = 1, 2, \ldots$. In CS, matrix $\boldsymbol{A_0}$ is symmetric semi-positive definite, so matrices $\boldsymbol{A_n}$ are all symmetric semi-positive definite for $n = 1, 2, \ldots$.

Theorem 3.1: For $n = 1, 2, \ldots$, $\mathcal{K}(\boldsymbol{A_n})$ are the condition number of the matrix $\boldsymbol{A_n}$, if $a_n > 1$, then

$$\mathcal{K}(\boldsymbol{A_n}) < \mathcal{K}(\boldsymbol{A_{n-1}}), \tag{8}$$

and

$$\lim_{n \to \infty} \mathcal{K}(\boldsymbol{A_n}) = 1. \tag{9}$$

Proof: In [25], it has been proven that (8) and (9) hold for $1 < a_n < 2$. Next, we will only discuss the case of $a_n \geq 2$. Denote $\{\mu_{n,k}\}_{k=1}^{n_1}$ with the algebraic multiplicity p_k be the decreasing positive eigenvalue sequence of $\boldsymbol{A_n}$, and $\{\boldsymbol{u_{j,k}}\}_{k=1}^{n_1}$ $(j = 1, 2, \cdots p_k)$ be the corresponding eigenvectors. Denote 0 is the eigenvalue of $\boldsymbol{A_n}$ with an algebraic multiplicity q, and $\boldsymbol{v_j}$ be the corresponding eigenvectors for $1 \leq j \leq q$. Let $\boldsymbol{U} = (\boldsymbol{U_1}, \boldsymbol{U_2}, \cdots, \boldsymbol{U_{n_1}}, \boldsymbol{V})$, where $\boldsymbol{V} = (\boldsymbol{V_1}, \boldsymbol{V_2}, \cdots, \boldsymbol{V_q})$ and $\boldsymbol{U_k} = (\boldsymbol{u_{1,k}}, \boldsymbol{u_{2,k}}, \cdots, \boldsymbol{u_{p_k,k}})$ for $k = 1, 2, \cdots n_1$. Then by (7c), the matrices $\boldsymbol{A_{n-1}}$ and $\boldsymbol{A_n}$ can be diagonalized into

$$\boldsymbol{U^T A_{n-1} U} = diag \left(\mu_{n-1,1} \boldsymbol{I_{p_1}}, \cdots, \mu_{n-1,n_1} \boldsymbol{I_{p_{n_1}}}, \boldsymbol{O_q} \right)$$

and

$$\boldsymbol{U^T A_n U} = diag \left((a_n \mu_{n-1,1} - \mu_{n-1,1}) \mu_{n-1,1} \boldsymbol{I_{p_1}}, \cdots, (a_n \mu_{n-1,1} - \mu_{n-1,n_1}) \mu_{n-1,n_1} \boldsymbol{I_{p_{n_1}}}, \boldsymbol{O_q} \right) \tag{10}$$

respectively, where $\boldsymbol{O_q}$ is the q-order null matrix. If we let

$$\begin{aligned}\mu_{n,k}(t) &= (a_n\mu_{n-1,1} - t)t \\ &= \frac{a_n^2\mu_{n-1,1}^2}{4} - \left(t - \frac{a_n\mu_{n-1,1}}{2}\right)^2, \end{aligned} \quad (11)$$

the positive eigenvalues, $\mu_{n,k}$, of the matrix $\boldsymbol{A_n}$ are $\mu_{n,k}(\mu_{n-1,1}), \cdots, \mu_{n,k}(\mu_{n-1,n_1})$. For $a_n \geq 2$, by (11), $\mu_{n,k} > 0$ and

$$\mu_{n-1,n_1} < \mu_{n-1,1} < \frac{a_n\mu_{n-1,1}}{2}.$$

Then by (11), we have

$$\max \mu_{n,k} = (a_n u_{n-1,1} - \mu_{n-1,1})\mu_{n-1,1} \quad (12)$$

and

$$\min \mu_{n,k} = (a_n u_{n-1,1} - \mu_{n-1,n_1})\mu_{n-1,n_1}. \quad (13)$$

So

$$\begin{aligned}\mathcal{K}(\boldsymbol{A_n}) &= \frac{\max\mu_{n,k}}{\min\mu_{n,k}} = \frac{(a_n u_{n-1,1} - \mu_{n-1,1})\mu_{n-1,1}}{(a_n u_{n-1,1} - \mu_{n-1,n_1})\mu_{n-1,n_1}} \\ &= \frac{a_n u_{n-1,1} - \mu_{n-1,1}}{a_n u_{n-1,1} - \mu_{n-1,n_1}}\mathcal{K}(\boldsymbol{A_{n-1}}) \\ &< \mathcal{K}(\boldsymbol{A_{n-1}}). \end{aligned} \quad (14)$$

Thus the inequality (8) still holds for $a_n \geq 2$.

According to the inequality (8), we know $\mathcal{K}(\boldsymbol{A_n})$ is monotonically decreasing with respected to weighting times n and greater than or equal to 1. By the monotone bounded theorem of the number sequence, the limit of $\mathcal{K}(\boldsymbol{A_n})$ exists and we assume

$$\lim_{n\to\infty} \mathcal{K}(\boldsymbol{A_n}) = \beta \geq 1. \quad (15)$$

By (14), for $a_n \geq 2$,

$$\begin{aligned}\mathcal{K}(\boldsymbol{A_n}) &= \frac{a_n u_{n-1,1} - \mu_{n-1,1}}{a_n u_{n-1,1} - \mu_{n-1,n_1}}\mathcal{K}(\boldsymbol{A_{n-1}}) \\ &= \frac{(a_n - 1)\mathcal{K}(\boldsymbol{A_{n-1}})^2}{a_n\mathcal{K}(\boldsymbol{A_{n-1}}) - 1} \\ &= \frac{(a_n - 1)\beta^2}{a_n\beta - 1}. \end{aligned} \quad (16)$$

Combining the (15) and (16), for $a_n \geq 2$, we have

$$1 \leq \beta = \frac{(a_n - 1)\beta^2}{a_n\beta - 1}. \quad (17)$$

The (17) holds only for $\beta = 1$ and the equality holds, otherwise if $\beta = 1 + \varepsilon > 1$, then

$$\begin{aligned}\frac{(a_n - 1)\beta^2}{a_n\beta - 1} &= \frac{(a_n - 1)(1+\varepsilon)^2}{a_n(1+\varepsilon) - 1} \\ &< \frac{(a_n - 1)(1+\varepsilon)^2}{a_n(1+\varepsilon) - 1 - \varepsilon} \\ &= \frac{(a_n - 1)(1+\varepsilon)^2}{(a_n - 1)(1+\varepsilon)} \\ &= 1 + \varepsilon = \beta, \end{aligned} \quad (18)$$

and this is contradictory with (17). So $\beta = 1$ and (9) holds for $a_n \geq 2$. Then the Theorem 3.1 is complete. ■

Let $\boldsymbol{D_0} = \boldsymbol{AA^T}$ and $\boldsymbol{D_n} = (a_{n-1}\varphi_{n-1}\boldsymbol{I} - \boldsymbol{D_{n-1}})\boldsymbol{D_{n-1}}$, where φ_{n-1} be the maximum eigenvalue of $\boldsymbol{D_{n-1}}$. By the (7c) and the theorem of SVD, a new sensing matrix, $\boldsymbol{\Psi_n}$, and the new observed data, $\boldsymbol{b_n}$, can be obtained. Obviously, $\boldsymbol{\Psi_n}$ satisfies $\boldsymbol{\Psi_n^T\Psi_n} = \boldsymbol{A_n}$ and $\boldsymbol{\Psi_n\Psi_n^T} = \boldsymbol{D_n}$. Then the sensing process (1) can be written equivalently as

$$\boldsymbol{\Psi_n x} = \boldsymbol{b_n}, \quad (19)$$

where $\boldsymbol{\Psi_n}$ can be regarded as the equivalent sensing matrix, obviously, $\boldsymbol{\Psi_0} = \boldsymbol{A}$. We need to recover $\boldsymbol{x}$ from (19).

Theorem 3.2: For the new sensing matrices $\boldsymbol{\Psi_n}$ in (19), $s \leq r$ and $n \geq 1$, if

$$\frac{\mu_{n-1,1}}{\mu_{n-1,s}} > \frac{\mu^s_{\max}(\boldsymbol{\Psi_n})}{\|\boldsymbol{\omega_{T_0}}\|_2^2\mu^s_{\min}(\boldsymbol{\Psi_n})}, \quad (20)$$

then

$$\delta_s(\boldsymbol{\Psi_{n-1}}) > \delta_s(\boldsymbol{\Psi_n}). \quad (21)$$

Proof: For $n = 1, 2, \cdots$, denote the SVD of $\boldsymbol{\Psi_n}$ as

$$\boldsymbol{\Psi_n} = \bar{\boldsymbol{U}}_n \begin{pmatrix} \boldsymbol{S_n} & \boldsymbol{0} \\ \boldsymbol{0} & \boldsymbol{0} \end{pmatrix} \bar{\boldsymbol{V}}_n^T, \quad (22)$$

where $\boldsymbol{S_n} = diag\left\{\sigma_{n,1}, \sigma_{n,2}, \cdots, \sigma_{n,r}\right\}$ and the positive singular values satisfy $\sigma_{n,1} \geq \sigma_{n,2} \geq \cdots \geq \sigma_{n,r} > 0$. By Theorem 2.2, we have

$$\frac{\mu^s_{\max}(\boldsymbol{\Psi_{n-1}})}{\mu^s_{\min}(\boldsymbol{\Psi_{n-1}})} > \frac{\mu^s_{\max}(\boldsymbol{\Psi_n})}{\mu^s_{\min}(\boldsymbol{\Psi_n})} \quad (23)$$

if

$$\frac{\sigma_{n-1,1}}{\sigma_{n-1,s}} > \frac{1}{\|\boldsymbol{\omega_{n-1,T_0}}\|_2}\sqrt{\frac{\mu^s_{\max}(\boldsymbol{\Psi_n})}{\mu^s_{\min}(\boldsymbol{\Psi_n})}}, \quad (24)$$

where $T_0 = \arg\max_{|T|=s}\left\{\|\boldsymbol{\omega_{n-1,T}}\|_2\right\}$ and $\boldsymbol{\omega_{n-1}}$ is the first row of $\bar{\boldsymbol{V}}_{n-1}^T$. By the (7c) and the theorem of SVD, we have $\bar{\boldsymbol{V}}_{n-1}^T = \bar{\boldsymbol{V}}_{n-2}^T = \cdots = \bar{\boldsymbol{V}}_0^T = \bar{\boldsymbol{V}}^T$ and $\boldsymbol{\omega_{n-1,T_0}} = \boldsymbol{\omega_{n-2,T_0}} = \cdots = \boldsymbol{\omega_{0,T_0}} = \boldsymbol{\omega_{T_0}}$. In addition, $\sigma_{n-1,1}^2 = \mu_{n-1,1}$ and $\sigma_{n-1,s}^2 = \mu_{n-1,s}$, so (24) can be transform into (20). Thus, under the condition (20), then (23) holds, and then by the Theorem 2.1, $\delta_s(\boldsymbol{\Psi_{n-1}}) > \delta_s(\boldsymbol{\Psi_n})$. ■

Obviously, $\boldsymbol{\Psi_n}$ and $\boldsymbol{A_n}$ have the same condition number, then by Theorem 3.1, the condition number of $\boldsymbol{\Psi_n}$ also decreases strictly monotonically to 1 as $n \to +\infty$. Besides, by Theorem 3.2, the RIC is improved under the condition (20). Note that the weighting times n may be increased appropriately according to the actual recovery requirement, but it cannot be very large to trade off between the improvement of RIC and the errors generated by discretization and accumulated with the increase of the weighting times n.

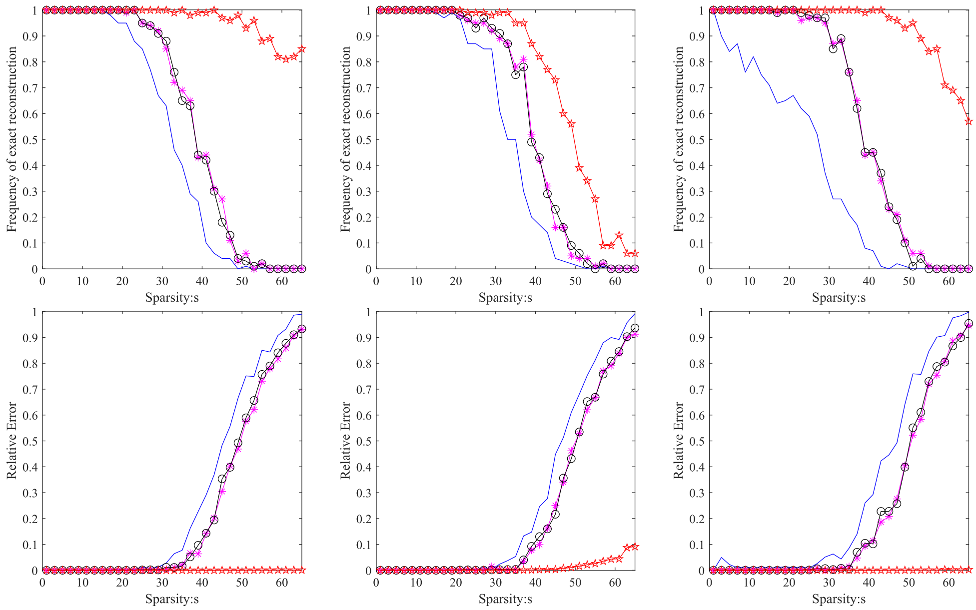

FIGURE 1. The reconstruction results of OMP (blue), SVD-WOMP (purple) and RE-WOMP (black: the weighting times $n = 9$, red: the weighting times $n = 32$ in left and $n = 33$ in middle and right). Left: Gaussian random matrix. Middle: Toeplitz matrix. Right: uniform random matrix.

IV. EXPERIMENT

In this section, to compare the reconstruction effects of the different recovery algorithms, we implement the CS experiments of one-dimensional s sparse signal recovery and two-dimensional CT reconstruction in subsection (IV-A) and (IV-B) respectively.

For the sake of illustration, the SVD-based weighted OMP, IHT and $L_{1/2}$R recovery algorithms of [14] are denoted by SVD-WOMP, SVD-WIHT and SVD-W$L_{1/2}$R respectively. The reweighted OMP, IHT and $L_{1/2}$R recovery algorithms of this article are denoted by RE-WOMP, RE-WIHT and RE-W$L_{1/2}$R respectively. In the above frameworks, if replacing the sensing matrix $\boldsymbol{A}$ by $\boldsymbol{A}_{\mathbf{svd}}$ and the observed data $\boldsymbol{y}$ by $\begin{pmatrix} \boldsymbol{S}^{-1} & \mathbf{0} \\ \mathbf{0} & \boldsymbol{I} \end{pmatrix} \bar{\boldsymbol{U}}^{\boldsymbol{T}} \boldsymbol{y}$, the SVD-WOMP, SVD-WIHT and SVD-W$L_{1/2}$R algorithms can be obtained. If replacing the sensing matrix $\boldsymbol{A}$ by $\boldsymbol{\Psi_n}$ and the observed data $\boldsymbol{y}$ by $\boldsymbol{b_n}$, we can get the RE-WOMP, RE-WIHT and RE-W$L_{1/2}$R algorithms.

A. ONE-DIMENSIONAL SPARSE SIGNAL RECOVERY

In the following CS experiments, we set the number of the observed data $\boldsymbol{y}$, $M = 120$, and the length of the sparse signal $\boldsymbol{x}$, $N = 512$. For the initial sensing matrix $\boldsymbol{A}$ in (1), we choose Gaussian random matrix, Toeplitz matrix and uniform random matrix differently. Note that the selected uniform random matrix may not be with a small δ_s. For the recovery algorithm, we use OMP [7], IHT [8] and $L_{1/2}$R algorithm [9] to recover the one-dimensional s sparse signal. We take sparsity $s = 1, 3, 5 \cdots, 65$ in Fig. 1, Fig. 2 and Fig. 3. For every sparsity s, we compute the frequency of exact reconstruction by reconstructing repeatedly the 100 different random s sparse signals satisfying Gaussian distribution. We define the relative error between the original signals $\boldsymbol{x}$ and the reconstruction results $\bar{\boldsymbol{x}}$ by

$$\text{Relative Error} := \frac{\| \boldsymbol{x} - \bar{\boldsymbol{x}} \|_2}{\| \boldsymbol{x} \|_2}. \tag{25}$$

The frequency of exact reconstruction and the relative error are two important indexes to evaluate the reconstruction effect, and the results are shown in Figs. 1-3 respectively.

From Figs. 1-3, obviously, the direct reconstruction effects of the OMP (IHT and $L_{1/2}$R) are worst. For the RE-WOMP (RE-WIHT and RE-W$L_{1/2}$R) with the weighting times $n = 9$, its reconstruction effects be near to that of the SVD-WOMP (SVD-WIHT and SVD-W$L_{1/2}$R). Besides, the frequency of the exact reconstruction and the relative error can be improved significantly by the RE-WOMP (RE-WIHT and RE-W$L_{1/2}$R) with the weighting times $n = 31, 32$ and 33 compared to the OMP (IHT and $L_{1/2}$R) and the SVD-WOMP (SVD-WIHT and SVD-W$L_{1/2}$R).

In the left and right columns of Fig. 1 with the sparsity $50 < s < 65$ (the left and right columns of Fig. 2 with the sparsity $40 < s < 45$, the middle and right columns of Fig. 3 with the sparsity $45 < s < 55$ and $40 < s < 50$), it is almost impossible for the OMP (IHT, $L_{1/2}$R) and the SVD-WOMP (SVD-WIHT, SVD-W$L_{1/2}$R) to reconstruct efficiently an one-dimensional s sparse signal, but it is possible for the RE-WOMP (RE-WIHT, RE-W$L_{1/2}$R).

B. APPLICATION TO CT RECONSTRUCTION

Next, we will conduct the CS experiments in CT. CT reconstruction is to invert an image function $\boldsymbol{X}(u, v)$,

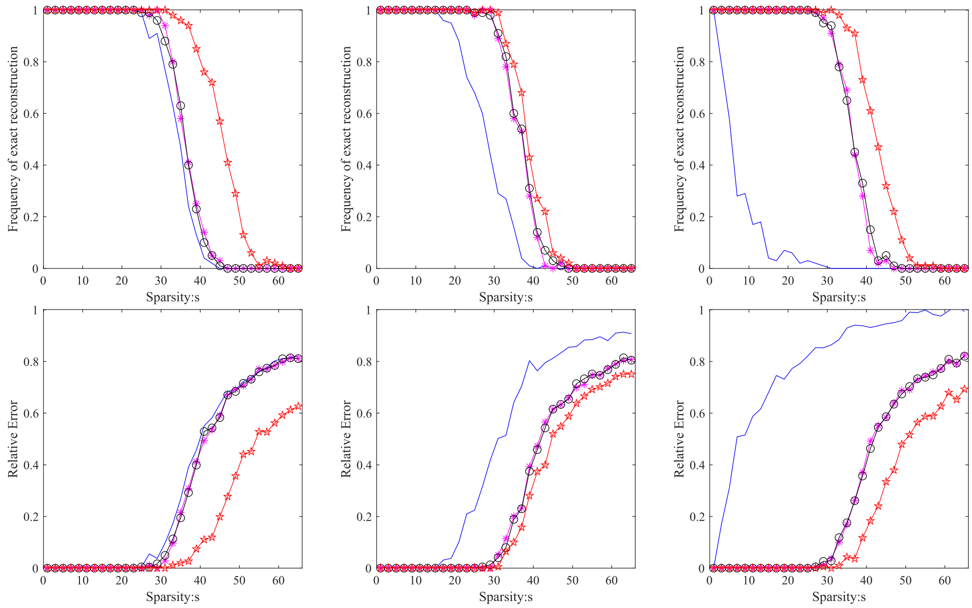

FIGURE 2. **The reconstruction results of IHT (blue), SVD-WIHT (purple) and RE-WIHT (black: the weighting times $n = 9$, red: the weighting times $n = 31$ in left and $n = 32$ in middle and right). Left: Gaussian random matrix. Middle: Toeplitz matrix. Right: uniform random matrix.**

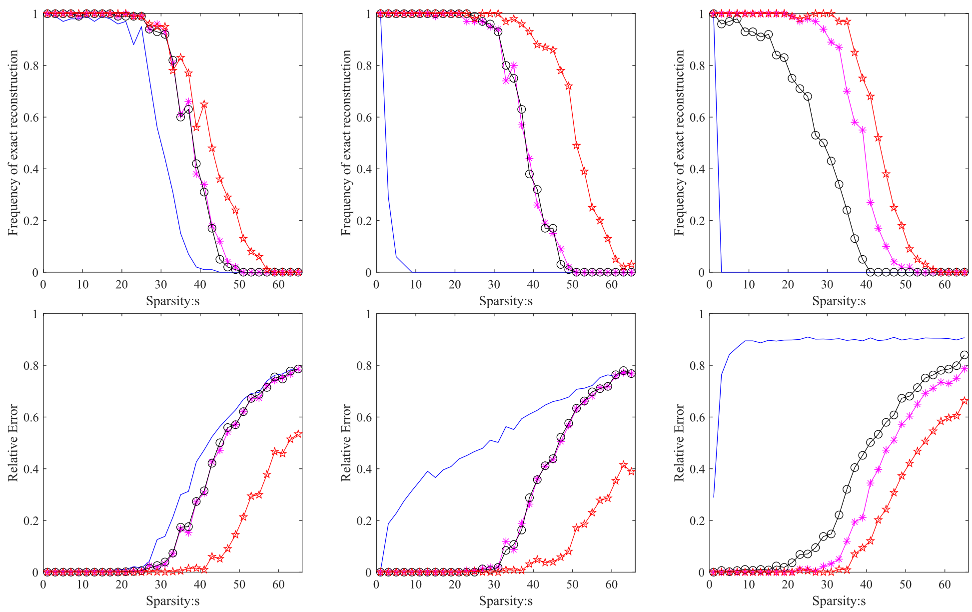

FIGURE 3. **The reconstruction results of $L_{1/2}R$ (blue), SVD-W$L_{1/2}R$ (purple) and RE-W$L_{1/2}R$ (black: the weighting times $n = 9$, red: the weighting times $n = 31$ in left, $n = 33$ in middle and $n = 32$ in right). Left: Gaussian random matrix. Middle: Toeplitz matrix. Right: uniform random matrix.**

$\text{supp}(\boldsymbol{X}) \in [0, 1] \times [0, 1]$, from the Radon transform [27],

$$\boldsymbol{Y}(p, \theta) = \int_{\ell: p = u\cos\theta + v\sin\theta} \boldsymbol{X} d\ell, \qquad (26)$$

where p is the distance the $X-$ray ℓ from the origin, θ is the angle between the u-axis and the normal of ℓ and $\boldsymbol{Y}(p, \theta)$ is the known projection data. By Partitioning $[0, 1] \times [0, 1]$ into $N = N_1 \times N_1$ square cells on an average, the continuous image $\boldsymbol{X}(u, v)$ can be discretized approximately as $\boldsymbol{X}(u_\iota, v_t)$ where $\iota, t = 1, 2, \cdots, N_1$. Let $j = (t-1)N_1 + \iota$, $1 \leq j \leq N$, $\boldsymbol{X}(u_\iota, v_t)$ can be rearranged as $\{x_j\}_{j=1}^{N}$. Let a_{ij} be the secant length of the ray i within the jth cell, where $i = 1, \cdots M$ and $j = 1, \cdots N$, and denote $\boldsymbol{A} = [a_{ij}]_{M \times N}$ be the projection matrix, then the projection process of CT is

$$\boldsymbol{A}\boldsymbol{x} = \boldsymbol{y}. \qquad (27)$$

Since in CT, $\boldsymbol{x}$ is usually not sparse, in order to apply CS to CT, we first calculate the sparse representation of $\boldsymbol{x}$ by using

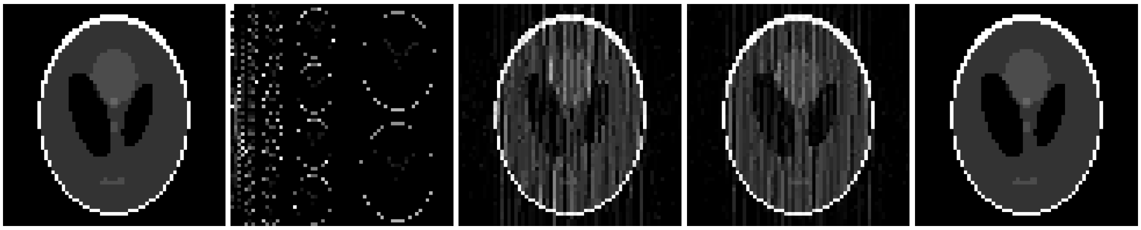

FIGURE 4. Reconstruction results. The first is the original image, the second is the sparse image after wavelet transform, the third is the image reconstructed by the OMP (PSNR=20.5912db, SSIM=0.6147), the fourth is the image reconstructed by the SVD-WOMP (PSNR=23.6668db, SSIM=0.6852), the last is the image reconstructed by the RE-WOMP with the weighting times $n = 27$ (PSNR=262.5134db, SSIM=1).

the following Haar wavelet with the mother wavelet $\Phi(z)$ and the scaling function $\phi(z)$, where $z \in \mathbb{C}$,

$$\Phi(z) = \begin{cases} 1 & 0 \le z < \frac{1}{2} \\ -1 & \frac{1}{2} \le z < 1 \\ 0 & \text{else} \end{cases}, \phi(z) = \begin{cases} 1 & 0 \le z < 1 \\ 0 & \text{else} \end{cases}. \quad (28)$$

Their translation and dilation are defined by

$$\Phi_i^j(z) := 2^{j/2}\Phi(2^j z - i) \text{ and } \phi_i^j(z) := 2^{j/2}\phi(2^j z - i)$$

differently, where $j \ge 1, 0 \le i \le 2^j - 1$.

Setting $u_\iota = \frac{2\iota-1}{2N_1}$ and $v_t = \frac{2t-1}{2N_1}$ for $\iota, t = 1, 2, \cdots, N_1$, then by per wavelet theory, x_j can be decomposed into [14]

$$x_j = \sum_{i=0}^{1} c_i^1 \phi_i^1 \left(\frac{2t-1}{2N_1^2}\right) + \sum_{k=1}^{j} \sum_{i=0}^{2^k-1} d_i^k \Phi_i^k \left(\frac{2t-1}{2N_1^2}\right) = \boldsymbol{\omega_t s^T},$$

where

$$\boldsymbol{\omega_t} = \left[\phi_0^1\left(\frac{2t-1}{2N_1^2}\right), \phi_1^1\left(\frac{2t-1}{2N_1^2}\right), \Phi_0^1\left(\frac{2t-1}{2N_1^2}\right), \right. \times \Phi_1^1\left(\frac{2t-1}{2N_1^2}\right), \cdots, \Phi_0^j\left(\frac{2t-1}{2N_1^2}\right), \cdots, \left. \times\ \Phi_{2^j-1}^j\left(\frac{2t-1}{2N_1^2}\right)\right]$$

and $\boldsymbol{s^T} = [c_0^1, c_1^1, d_0^1, d_1^1, \cdots, d_0^j, \cdots, d_1^j]$. Let $\boldsymbol{H}$ be discrete Haar wavelet transform matrix and $\boldsymbol{\omega_t}$ be its tth row, then

$$\boldsymbol{x} = \boldsymbol{H}\bar{\boldsymbol{x}}, \quad (29)$$

where $\bar{\boldsymbol{x}}$ is the sparse representation of $\boldsymbol{x}$. Thus, the sensing process (1) can be rewritten as

$$\boldsymbol{AH}\bar{\boldsymbol{x}} = \boldsymbol{y}. \quad (30)$$

Now, $\boldsymbol{AH}$ is the sensing matrix, we reconstruct $\bar{\boldsymbol{x}}$ by (30), and then get $\boldsymbol{x}$ through (29).

In the following experiments, the original image is the Shepp-Logan phantom with the size of 64×64. We use a parallel beam scan projection of 20 different angles with 95 rays per projection. Hence, the sensing matrix $\boldsymbol{A}$ is the size of 1900×4096. We obtain $\boldsymbol{A}$ by using the method of [28], and then reconstruct $\boldsymbol{x}$ by the OMP, the SVD-WOMP of [14], and the RE-WOMP of this article differently.

TABLE 1. The PSNR and SSIM of the results reconstructed by the RE-WOMP with the weighting times $n = 27$.

SNR	PSNR	SSIM
30db	36.8422db	0.9231
35db	38.0431db	0.9522
40db	39.0895db	0.9802
45db	47.8337db	0.9944
50db	51.9847db	0.9987

The reconstruction results are shown in Fig. 4, where the last reconstructed image is very close to the original image and the third and fourth reconstructed images have very high levels of artifacts.

In order to investigate the sensitivity of the RE-WOMP of this article to noise, we add the White Gaussian noises of different levels to the observed data (simulation projection data), $\boldsymbol{y}$, and implement reconstruction. We use the signal-to-noise ratio (SNR) to measure the noise level in $\boldsymbol{y}$, and the quantitative evaluation results are given in Table. 1.

V. CONCLUSION

In this article, we have established a complete theoretical analysis of improving RIC for the reweighted method and got an RIC improvement CS model (19). We have also implemented the CS experiments of the general one-dimensional sparse signal recovery and the two-dimensional CT reconstruction, and verified the superiority of our algorithms by comparing with the direct recovery algorithms and the algorithms of [14]. In some fields, such as the general imaging problem, the application of CS is restricted from their fixed sensing matrix with a large RIC. The reweighted method proposed in this article can improve the RIC to ensure the exact recovery of sparse signals, so it expands the application field of CS.

ACKNOWLEDGMENT

The authors would like to thank the editor and the reviewers for their detailed comments and valuable suggestions.

REFERENCES

[1] S. Foucart and H. Rauhut, *A Mathematical Introduction to Compressive Sensing*. Boston, MA, USA: Birkhäuser, 2013, pp. 1–8.

[2] L. C. Potter, E. Ertin, J. T. Parker, and M. Cetin, "Sparsity and compressed sensing in radar imaging," *Proc. IEEE*, vol. 98, no. 6, pp. 1006–1020, Jun. 2010.

[3] D. Valsesia, G. Coluccia, and E. Magli, "Graded quantization for multiple description coding of compressive measurements," *IEEE Trans. Commun.*, vol. 63, no. 5, pp. 1648–1660, May 2015.

[4] X. Zou, L. Feng, and H. Sun, "Robust compressive sensing of multichannel EEG signals in the presence of impulsive noise," *Inf. Sci.*, vol. 429, pp. 120–129, Mar. 2018.

[5] S. Khanna and C. R. Murthy, "On the restricted isometry of the column-wise KhatriíCRao product," *IEEE Trans. Signal Process.*, vol. 66, no. 5, pp. 1170–1183, Mar. 2018.

[6] L. Feng, H. Sun, and J. Zhu, "Robust image compressive sensing based on half-quadratic function and weighted schatten-p norm," *Inf. Sci.*, vol. 477, pp. 265–280, Mar. 2019.

[7] Y. C. Pati, R. Rezaiifar, and P. S. Krishnaprasad, "Orthogonal matching pursuit: Recursive function approximation with applications to wavelet decomposition," in *Proc. 27th Asilomar Conf. Signals, Syst. Comput.*, Nov. 1993, pp. 40–44.

[8] T. Blumensath and M. E. Davies, "Iterative hard thresholding for compressed sensing," *Appl. Comput. Harmon. Anal.*, vol. 27, no. 3, pp. 265–274, Nov. 2009.

[9] Z. Xu, X. Chang, F. Xu, and H. Zhang, "$L_{1/2}$ regularization: A thresholding representation theory and a fast solver," *IEEE Trans. Neural Netw. Learn. Syst.*, vol. 23, no. 7, pp. 1013–1027, Jul. 2012.

[10] R. Wu and D.-R. Chen, "The improved bounds of restricted isometry constant for recovery via ℓ_p -Minimization," *IEEE Trans. Inf. Theory*, vol. 59, no. 9, pp. 6142–6147, Sep. 2013.

[11] M. Jing, X. Zhou, and C. Qi, "Quasi-Newton iterative projection algorithm for sparse recovery," *Neurocomputing*, vol. 144, pp. 169–173, Nov. 2014.

[12] M. Rudelson and R. Vershynin, "Sparse reconstruction by convex relaxation: Fourier and Gaussian measurements," in *Proc. 40th Annu. Conf. Inf. Sci. Syst.*, Mar. 2006, pp. 207–212.

[13] C.-B. Song, S.-T. Xia, and X.-J. Liu, "Improved analysis for subspace pursuit algorithm in terms of restricted isometry constant," *IEEE Signal Process. Lett.*, vol. 21, no. 11, pp. 1365–1369, Nov. 2014.

[14] Q. Wang and G. Qu, "Restricted isometry constant improvement based on a singular value decomposition-weighted measurement matrix for compressed sensing," *IET Commun.*, vol. 11, no. 11, pp. 1706–1718, Aug. 2017.

[15] H. Ge, L. Wang, J. Wen, and J. Xian, "An RIP condition for exact support recovery with covariance-assisted matching pursuit," *IEEE Signal Process. Lett.*, vol. 26, no. 3, pp. 520–524, Mar. 2019.

[16] J. Wang and P. Li, "Recovery of sparse signals using multiple orthogonal least squares," *IEEE Trans. Signal Process.*, vol. 65, no. 8, pp. 2049–2062, Apr. 2017.

[17] H. Li, J. Zhang, and J. Zou, "Improving the bound on the restricted isometry property constant in multiple orthogonal least squares," *IET Signal Process.*, vol. 12, no. 5, pp. 666–671, Jul. 2018.

[18] H. Liu, J. Peng, and Z. Lin, "A theoretical result of sparse signal recovery via alternating projection method," *Inf. Sci.*, vol. 506, pp. 51–57, Jan. 2020.

[19] E. J. Candes and T. Tao, "Decoding by linear programming," *IEEE Trans. Inf. Theory*, vol. 51, no. 12, pp. 4203–4215, Dec. 2005.

[20] V. Abolghasemi, S. Ferdowsi, B. Makkiabadi, and S. Sanei, "On optimization of the measurement matrix for compressive sensing," in *Proc. 18th Eur. Signal Proces. Conf.*, Aalborg, Denmark, Aug. 2010, pp. 427–431.

[21] V. Saligrama, "Aperiodic sequences with uniformly decaying correlations with applications to compressed sensing and system identification," *IEEE Trans. Inf. Theory*, vol. 58, no. 9, pp. 6023–6036, Sep. 2012.

[22] B. Li, Y. Shen, and J. Li, "Dictionaries construction using alternating projection method in compressive sensing," *IEEE Signal Process. Lett.*, vol. 18, no. 11, pp. 663–666, Nov. 2011.

[23] B. Li, L. Zhang, T. Kirubarajan, and S. Rajan, "Projection matrix design using prior information in compressive sensing," *Signal Process.*, vol. 135, pp. 36–47, Jun. 2017.

[24] A. Ebian, B. Abdelhamid, and S. El-Ramly, "New measurement matrix for compressive sensing in cognitive radio networks," *IET Commun.*, vol. 12, no. 11, pp. 1297–1306, Jul. 2018.

[25] M. Chen, G. Qu, L. Shi, and S. Gao, "The reweighted landweber scheme for the extrapolation of band-limited signals," *Signal Process.*, vol. 164, pp. 340–344, Nov. 2019.

[26] M. F. Chen, G. R. Qu, and L. Shi, "A reweighted orthogonal matching pursuit method for blind multiband signal reconstruction (translation journals style)," *J. Univ. Shanghai Sci. Technol.*, vol. 3, pp. 240–246, 2020, doi: 10.13255/j.cnki.jusst.20191029005.

[27] F. Natterer, *The Mathematics of Computerized Tomography*. Hoboken, NJ, USA: Wiley, 1986, pp. 9–18.

[28] R. L. Siddon, "Fast calculation of the exact radiological path for a three-dimensional CT array," *Med. Phys.*, vol. 12, no. 2, pp. 252–255, Mar. 1985.

LEI SHI received the M.S. degree in applied mathematics from Beijing Information Science and Technology University, in 2017. He is currently pursuing the Ph.D. degree in computational mathematics with Beijing Jiaotong University, Beijing, China. His research interests include image reconstruction and compressed sensing.

GANGRONG QU received the B.S. degree in mathematics from Jilin University, Jilin, China, in 1983. He is currently a Professor with the School of Science, Beijing Jiaotong University. His research interests include image reconstruction and compressed sensing.

QIAN WANG received the Ph.D. degree in computational mathematics from Beijing Jiaotong University. She is currently a Lecturer with the School of Science, Tianjin University of Commerce. Her research interests include compressed sensing and phase retrieval.